Electrophoretic Deposition and Characterization of TiO 2 /Nb 2 O 5 Composite Thin Films for Dye Sensitized Solar Cells

4 authors:

John Nguu
University of Nairobi
10 PUBLICATIONS **13** CITATIONS

SEE PROFILE

Francis Nyongesa
University of Nairobi
18 PUBLICATIONS **61** CITATIONS

SEE PROFILE

Robinson Musembi
University of Nairobi
44 PUBLICATIONS **115** CITATIONS

SEE PROFILE

B. O. Aduda
University of Nairobi
56 PUBLICATIONS **294** CITATIONS

SEE PROFILE

Some of the authors of this publication are also working on these related projects:

Project   electrochemical impedance spectroscopy View project

Project   Microstructure - Material property relationships in materials (ceramics, composites) View project

Electrophoretic Deposition and Characterization of TiO$_2$/Nb$_2$O$_5$ Composite Thin Films for Dye Sensitized Solar Cells

John Nguu, Francis Nyongesa[*], Robinson Musembi, Bernard Aduda

Department of Physics, University of Nairobi, P.O. Box 30197-00100, Nairobi, Kenya
*Corresponding author: fnyongesa@uonbi.ac.ke

Abstract In this study, Electrophoretic Deposition (EPD) technique was used to fabricate TiO$_2$/Nb$_2$O$_5$ composite thin films on FTO coated glass for application as photoelectrodes in Dye Sensitized Solar Cells (DSSC). A TiO$_2$/Nb$_2$O$_5$ ratio of 1:1 was used in a 2-propanol suspension solution with a solid loading of 0.25g/L. Optical investigations showed that the film with thickness of 5.5 μm deposited at 35.0 V for 90.0 s had the highest transmittance of 55.0 % at a wavelength (λ) of 1,300 nm. The optical band gap energy (E_g) was 3.884 eV and was found to be dependent on the annealing time. The solar cell fabricated from this film had an open circuit voltage (V_{OC}) of 0.66 V, fill factor (*FF*) of 57.0%, short current density (J_{SC}) of 5.25 mA/cm^2 and photo conversion efficiency (PCE) of 2.0%. Electrochemical Impedance Spectroscopy (EIS) analysis indicate that the DSSC device with thinner photoelectrodes have more efficient electron transport in the photoanode compared to thicker photoelectrodes to achieve higher conversion efficiencies.

Keywords: *electrophoretic deposition, dye-sensitized solar cell, TiO$_2$/Nb$_2$O$_5$ composite thin films*

Cite This Article: John Nguu, Francis Nyongesa, Robinson Musembi, and Bernard Aduda, "Electrophoretic Deposition and Characterization of TiO$_2$/Nb$_2$O$_5$ Composite Thin Films for Dye Sensitized Solar Cells." *Journal of Materials Physics and Chemistry*, vol. 6, no. 1 (2018): 1-8. doi: 10.12691/jmpc-6-1-1.

1. Introduction

The continued consumption of fossil fuels poses challenge of depletion of these energy sources and affects climatic conditions due to CO2 emission. One strategy has been to invest in renewable energy generation using photovoltaic (PV) technologies. A lot of research is currently geared towards developing low cost PV solar cells with adequate conversion efficiencies [1]. Dye sensitized solar cell (DSSC) is among the emerging technologies that has gained widespread attention owing to their relatively low production costs, simple manufacturing techniques, great aesthetic features like colour, potential for indoor and outdoor applications and fair photon to electron energy conversion efficiencies [2]. A major component of a DSSC is the photoelectrode, whose function is to transmit light and inject electrons to an external circuit. A good photoelectrodes should have high optical transparency and good electrical conductivity [3], in order to achieve high conversion efficiency of a DSSC. Titanium (IV) oxide (TiO$_2$) is a key semi-conducting material for fabricating photoelectrodes since it was first successfully employed in 1991 by O'Regan and Gratzel for DSSCs [4]. To realize improvement in the efficiency of DSSCs, composite materials of TiO$_2$ and other metal oxides have been explored as well as several thin film deposition techniques.

Several studies have initiated to modify the electrical transport properties of TiO$_2$ using composite electrodes, core/shell structures, and doping with other metal oxides such as Nb$_2$O$_5$, ZnO, GeO$_2$, ZrO$_2$, SiO$_2$, Al$_2$O$_3$, MgO and SrTiO$_3$ [5]. When used in DSSCs, niobium oxide (Nb$_2$O$_5$) has both good absorption of Ru dyes as well as a higher conduction band which is 100 mV above the conduction band of TiO$_2$. This enhances charge separation and collection, with resultant effect of increased photo conversion efficiency (PCE) [5]. On the other hand, Doctor blade [6], spin coating [7], sputtering [8,9], dip coating [10], screen printing [11] and electrophoretic deposition (EPD) [12,13] are some of the methods used to manufacture titanium dioxide films. The EPD technique involves movement of charged particles in a suspension medium followed by deposition of the particles on a substrate under an applied DC voltage [14-21]. This technique has not been fully exploited in the fabrication of photoelectrodes for DSSCs despite its many advantages which include simple equipment, high reproducibility, rapid coating and low cost of film fabrication. Additionally, the EPD technique also offers easy manipulation of the thickness of deposited films via control of the deposition parameters and the deposition conditions such as the DC voltage and deposition time [22,23,24]. In the present work, the use of EPD technique is explored for the fabrication of mixed-particle TiO$_2$/Nb$_2$O$_5$ composites films for application in DSSCs.

2. Materials and Methods

2.1. Optimization of EPD Deposition Parameters

Commercial glass substrates (16.0 mm × 25.0 mm × 1.0 mm) coated with a conducting layer of fluorine doped tin oxide (FTO) (Pilkington, Inc., USA) having sheet resistances of 8.0 Ω/m^2 were used as electrodes in the EPD cell. The EPD suspension was created by dispersing 0.25g/L of commercial TiO_2 nanopowder (CAS No. 13463-67-7, Aldrich) and Nb_2O_5 nanopowder (CAS No. 1313-96-8, Acros Organics BVBA, Belgium) in the ratio 1:1 in 2-propanol (Scharlau Chemie) contained in a Pyrex beaker. 5.0 mg of $Mg(NO_3)_2$ pellets (Aldrich) were added to the EPD cell to form the electric charging system thereby controlling the zeta potential. The suspension was stirred for 1.0 h using a power sonicator (Sonic 405) before being used in the EPD cell. The EPD set up consisted of a cell (Pyrex glass beaker) and a DC power supply (Thurlby Thadar TS30225) with the electrodes partially immersed in suspension as shown in Figure 1. The cross section part of the substrate (cathode) and the counter electrode that was under the suspension was 1.6 x 1.5 cm^2 and they were placed 1.5 cm apart.
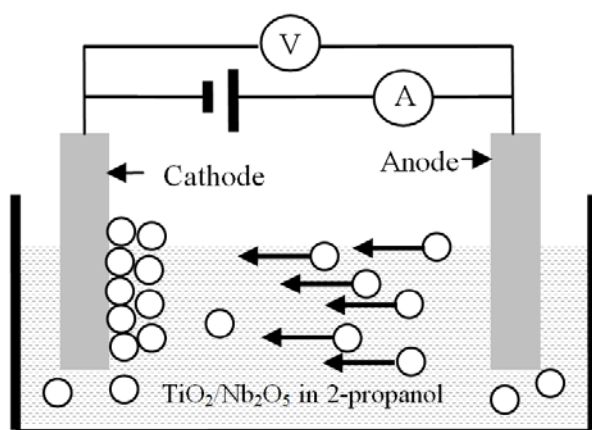

Figure 1. Schematic set-up of the EPD cell.

To achieve deposition, various DC voltages ranging from 15.0 – 60.0V were applied across the electrodes for various deposition times ranging from 60.0 to 180.0s. The films were then annealed at 450.0 °C for 3 – 6 hours at a heating rate of 5.0 °C per min to achieve good adhesion. Optimal deposition conditions of voltage and time were obtained from the analysis of the transmittance data through the films.

2.2. Optical Characterization of TiO_2/Nb_2O_5 Composite Films

Spectroscopic transmission measurements of the TiO_2/Nb_2O_5 films were carried out using Shimadzu-DUV spectrophotometer. The film thickness was measured using Micronstat FD/ND – coating-thickness with (FD/ND) G-22-type probe. Surface morphology was investigated using scanning electron microscope (SEM)

model S4100 HITACHI to determine the quality of the deposited films while sstructural analysis was conducted using Shimadzu X-Ray Diffractometer with Cu Kα radiation with a scanning range of 2θ from 10°-80°.

2.3. DSSC Assembly and Photovoltaic Characterization

The thin films for DSSC were chemisorbed with a dye (Ruthenium-dye solution (Ru – N719) of 0.5 mM) supplied by Sigma Aldrich. The dye solution was prepared by dissolving 6.0 mg of Ru-719 in 10.0 ml of ethanol and sonicated until thoroughly mixed. The TiO2/Nb2O5 composite films were preheated to 200.0 °C for 10.0 mins to remove adsorbed water and thereafter soaked in the dye solution for 24 hours to enable proper dye chemisorptions. They were then washed with ethanol to remove unabsorbed dye molecules before being used as DSSC photoanodes. The DSSC electrolyte composed of an iodide/triiodide (I^-/I_3^-) red-ox couple was prepared by dissolving: 0.101 g (0.04 M) iodine (CAS 7553-56-2), 0.134 g (0.1M) lithium iodide (CAS 10377-51-2), and 1.477 g (0.5M) tetra-n-butylammonium iodide, in 10.0 ml of acetonitrile (CAS 75-05-8). The 4-tert-butylpyridine (CAS 3978-81-2) was added to electrolyte to increase the voltage output. The counter electrodes (CE) consisted of platinum(Pt)-coated catalyst and were prepared by evenly spreading drops of 5.0 mM hexachloroplatinic acid (H_2PtCl_6) (Fluka) on cleaned FTO glass and heating the FTO glass at 450.0 °C for 45.0 mins.

The cell was assembled by placing the platinum coated counter electrode (CE) over the dye-sensitized porous TiO_2/Nb_2O_5 composite photoelectrode to form a sandwich arrangement as shown in Figure 2. The edges of the cell were sealed by hot pressing the two electrodes together with a 25-μm thermal-plastic Surlyn spacer. A proper amount of liquid electrolyte was then injected in the gap between the two electrodes through small holes drilled in the counter electrode (CE). The holes were sealed using a piece of microscope covering plastic. The current and voltage characteristics of the cell were performed using a digital source meter (Keithley-2400) under simulated sunlight of one sun illumination (AM 1.5G, 100.0 mW/cm^2).
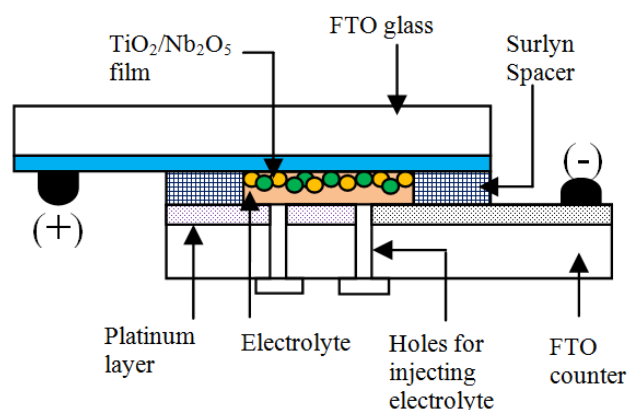

Figure 2. Assembly of dye sensitized cell based on TiO_2/Nb_2O_5 composite thin film

2.4. Electrochemical Impedance Spectroscopy (EIS) Measurement

The EIS measurements were performed using an AUTOLAB (PGSTAT204) equipment (Metrohm, Switzerland) in the frequency range 10.0 kHz to 0.1Hz by applying an AC amplitude of 5.0 to 15.0 mV. The sinusoidal current response was measured using the NOVA software and the impedance at each frequency computed. The biasing DC voltage of 0.5V was used in the EIS measurements because this value is approximately the V_{oc} of the fabricated solar cells. The real and imaginary parts of the impedance were then plotted to yield the Nyquist plot used to analyze the solar cell.

3. Results and Discussions

3.1. Optimized EPD Parameters for TiO$_2$/Nb$_2$O$_5$ Composites Films

Figure 3 shows the variation in film thickness of TiO2/Nb2O5 composites with deposition voltage at constant deposition time. It was observed that the film thickness increased, initially slowly (indicating a slow deposition rate) at lower voltages, followed a rapid growth in film thickness in the voltage range 30.0 - 55.0 V. This behaviour was attributed to increase in the dragging force (and hence higher charge mobility) with increase in DC voltage resulting in rapid deposition rate. However, at high deposition voltages (> 55.0 V), the growth in film thickness tended to plateau. This could be attributed to increase in the resistance of the film caused by formation of TiO$_2$/Nb$_2$O$_5$ agglomeration on the film as a result of high currents that cause rapid particle deposition. Subsequently, electrophoretic mobility reduced such that fewer particles reached the substrate and the deposit mass remains nearly constant with time. Similar observations were made for high EPD deposition voltages of TiO$_2$ particles [14,25].
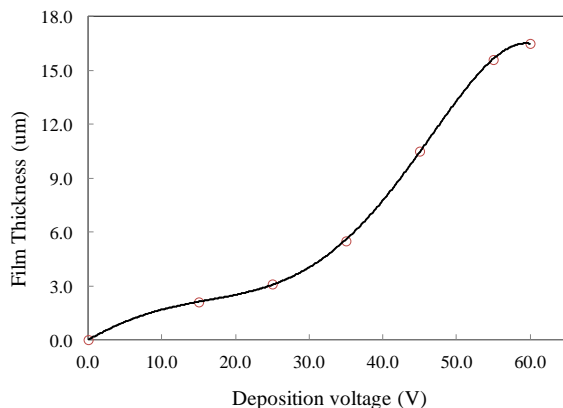

Figure 3. Variation in film thickness of TiO$_2$/Nb$_2$O$_5$ films with EPD deposition voltage

The optimized deposition voltage and hence the film thickness for DSSC, was obtained by studying the variation in the transmittance through films of various thickness as shown in Figure 4 using films annealed at 450.0 °C. It was observed that the transmittance of the films first increased (and hence light absorption decreased) with increase in film thickness reaching a peak at a film thickness of 5.5 μm and thereafter, it decreased with further increase in film thickness. The deposition voltage that corresponds to film thickness of 5.5 μm is 35.0 V (from Figure 3) with a deposition time of 90.0s. SEM micrographs of films deposited at 90.0s showed nearly uniform deposit mass before annealing (Figure 5a) while extended deposition times (> 90.0s) resulted in formation of agglomeration (Figure 5b). After annealing, micro cracks were observed in thicker films of 12.0 μm (Figure 5c) that were most probably caused by evaporation of the solvent during the annealing processes. Such micro cracks, combined with agglomerations, contribute to light scattering and absorption phenomena resulting in less transmittance in thicker films. Comparatively, thinner films of 5.5 μm showed absence of micro cracks (Figure 5d).
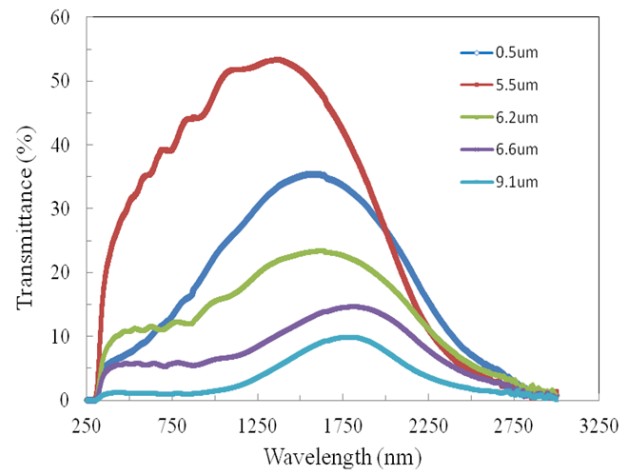

Figure 4. Variation of transmittance with wavelength in TiO$_2$/Nb$_2$O$_5$ composite films of various thicknesses deposited at 35.0 V for 90.0s.
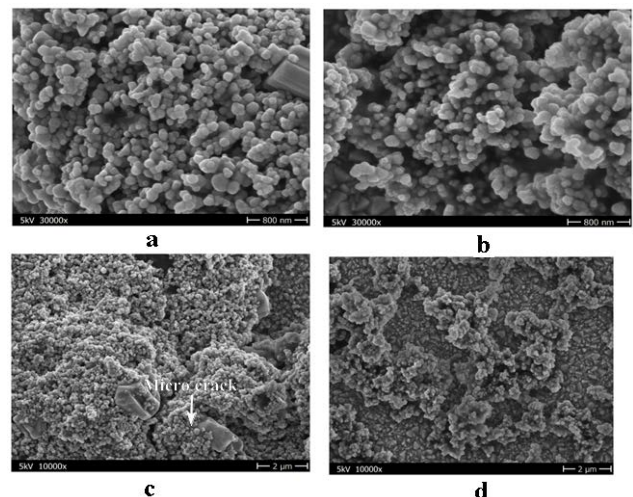

Figure 5. SEM images of TiO$_2$/Nb$_2$O$_5$ composite films (a) 5.5 μm film showing uniform coating before annealing, (b) 12.0 μm film before annealing showing agglomeration (c) 12.0 μm film showing micro cracks after annealing at 450.0°C and (d) 5.5 μm film showing absence of micro cracks after annealing

Notably, these agglomerations and micro cracks could also be responsible for the observed decrease and shifting of the transmittance peaks towards the long wavelengths

regions with increase in film thickness (Figure 4). As such, the transmitted photon has less energy (hence longer wavelength). The highest transmittance of 53% at $\lambda = 1,300.0$ nm was observed in films deposited at 90.0s at 35.0 V with film thickness of 5.5μm. This film thickness falls within typical TiO2 film thickness for DSSC which range between 5.0 - 15.0 μm [15]. Consequently, applied voltage of 35.0V and deposition time of 90.0s was chosen as the optimum EPD deposition conditions for the TiO_2/Nb_2O_5 composite thin films.

3.2. Photovoltaic Performance of DSSC

Figure 6 shows the photocurrent density - versus voltage (J - V) curves of the TiO_2/Nb_2O_5 composite photoelectrodes of varying thicknesses. It is observed that whereas the circuit voltage remains nearly constant at 0.66 V, the current density decreases with increase in film thickness. This behaviour is attributed to the decrease in the transmittance with increase in film thickness earlier observed in Figure 4, a phenomena that reduces the incident light intensity to the dyes. Further, since the charge transfer resistance increases with increase in film thickness, the charge recombination between electrons injected from the excited dye to the conduction band of TiO_2/Nb_2O_5 and the I_3^- ions in the electrolyte is higher in thicker films due to the long diffusion lengths such that most of the photoelectrons do not reach the FTO. These factors, in additionally to the defects such as clusters and micro-cracks observed in thicker films (Figure 5c), contribute to lowering the electron mobility in the film thereby resulting in reduced current density. The highest current density was obtained with a film thickness of 5.5 μm.
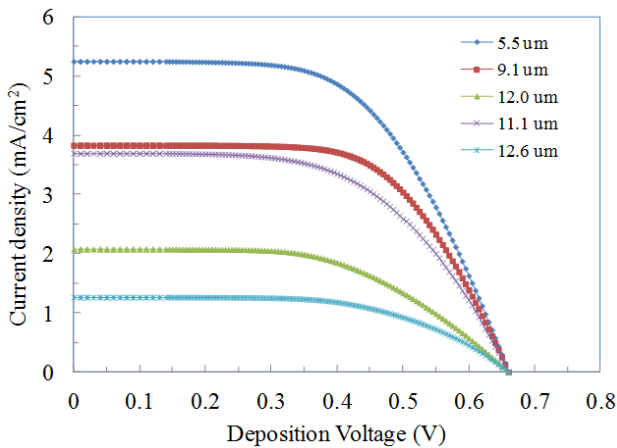

Figure 6. The photocurrent density – photovoltage (J – V) curves based on TiO_2/Nb_2O_5 composite thin films

The open-circuit voltage (V_{OC}), short-circuit current density (J_{SC}), fill-factor (FF), and energy conversion efficiency (η) were derived from the J–V curves of Figure 6 together with Eq. (1) and (2) respectively.

$$FF = \frac{P_{Max}}{P_{IN}} = \frac{J_{Max}V_{Max}}{J_{SC}V_{OC}} \qquad (1)$$

$$\eta = \frac{J_{SC}V_{OC}FF}{P_{IRR}} \qquad (2)$$

where V_{Max} is the maximum voltage, J_{Max} is the maximum current density (mA/cm^2) and P_{IRR} is the light intensity (mW/cm^2). Table 1 shows the solar cell characteristics (V_{OC}, J_{SC}, FF and cell efficiency, η) for photoelectrodes of various film thicknesses. It is observed that the photo conversion efficiency (η) decreases from a maximum of 2.0% to 0.1% respectively with increase in film thickness. This observation indicates that although thicker TiO_2/Nb_2O_5 composite films may adsorb relatively more of the dye molecules leading to enhancement in the photocurrent of the cell, thicker films are less transparent which negatively affect their light harvesting and performance of the DSSC since the current density and hence the photo conversion efficiency (η) decreases with increase in film thickness.

Table 1. DSSC characteristics of TiO_2/Nb_2O_5 composite thin films

EPD deposition time (s)	Film thickness (μm)	V_{OC} (V)	J_{SC} (mA/cm^2)	FF %	η (%)
90.0	5.5	0.66	5.25	0.57	2.0
120.0	6.2	0.63	3.83	0.61	1.5
150.0	6.6	0.69	2.08	0.55	0.8
180.0	9.1	0.66	1.80	0.58	0.7
240.0	12.1	0.58	0.13	0.65	0.1
270.0	12.0	0.65	0.23	0.59	0.1

Table 2 shows a comparison of DSSC parameters with other references [26,27,28]. Our experimental values compare well with those obtained by other authors for TiO_2/Nb_2O_5 composite structures. These results are also in agreement with observation made by other authors that N_2O_5 decreases the loss due to carrier recombination, i.e., it increases the shunt resistance resulting in increased FF and V_{OC} of composite electrode cells thereby enhancing the photo conversion efficiency [5,28].

Table 2. Comparison of DSSC parameters of TiO2/Nb2O5 composites with other references [26,27,28].

Film structure	V_{OC}	J_{SC}	FF (%)	η (%)	Ref
TiO_2/Nb_2O_5 composite	0.66	5.25	0.57	2.0	This study
$80TiO_2/20Nb_2O_5$ composite	0.645	6.83	0.42	1.9	[28]
$TiO_2/0.1\ Nb_2O_5$ (Doped)	0.841	3.1	0.69	1.8	[28]
TiO_2/Nb_2O_5 (core shell)	0.732	11.4	0.56	4.7	[28]
TiO_2/Nb_2O_5 (core shell)	0.730	11.4	0.51	4.9	[26]
TiO_2/Nb_2O_5	0.77	4.26	0.56	1.9	[27]

3.3. Evaluation of Optical Band Gap Energy

The Tauc model has been devised as an empirical model for determining the optical gap in semiconductors and gives the relationship between the absorption coefficient (α) to photon energy (hν) by Eq. (3) below [8].

$$(\alpha h\nu)^{\frac{1}{n}} = \beta(h\nu - E_g) \qquad (3)$$

where β is the band tailing parameter, E_g is the absorption band gap energy and n denotes the type of transition with $n = \frac{1}{2}$ for direct transitions and $n = 2$ for indirect transitions of anatase TiO_2 [29]. For crystalline materials, direct transitions are valid [8,29] and subsequently, for our present TiO_2/Nb_2O_5 thin films, $n = \frac{1}{2}$, hence, the tangent intercept in the Tauc plot of $(\alpha h\nu)^2$ versus $(h\nu)$ represents E_g.

Figure 7 shows a plot of $(\alpha h\nu)^2$ versus $h\nu$ used for evaluating the band gap of TiO_2/Nb_2O_5 composite thin films, pure TiO_2 (anatase) and pure Nb_2O_5 films. From the graph, the optical band gap energies for pure TiO_2 are 3.932 eV, pure Nb_2O_5 is 3.858 eV and for TiO_2/Nb_2O_5 composite is 3.884eV. The band gap energy values obtained for the composite film lie between that of pure TiO_2 and pure Nb_2O_5. Our experimental values are consistent with many authors who have reported Eg values of TiO_2 (anatase) in the range 3.25 – 4.14 eV [26,30,31,32,33,34] and E_g values of NbO_5 in the range 3.49 – 3.90 eV [35,36], but are slightly higher compared to the theoretical direct band gap value of anatase TiO_2 (E_g = 3.25 eV) [28] and Nb_2O_5 (E_g = 3.49 eV) [30] respectively. This difference between theoretical and our experimental E_g values of both pure TiO_2 and Nb_2O_5 films could be attributed to the development of sub-band gap states in the TiO_2/Nb_2O_5 composite films that lie deep in the tail of the density of states in the films and result in decreasing the optical energy gap and shifting the absorption edge towards the higher wavelength of the incident photons.
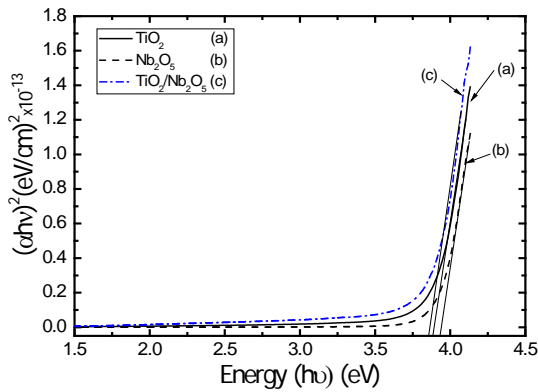

Figure 7. Variation of $(\alpha h\nu)^2$ versus $h\nu$ for direct band gap transitions in (a) TiO_2/Nb_2O_5 composite (b) TiO_2 and (c) Nb_2O_5 films.

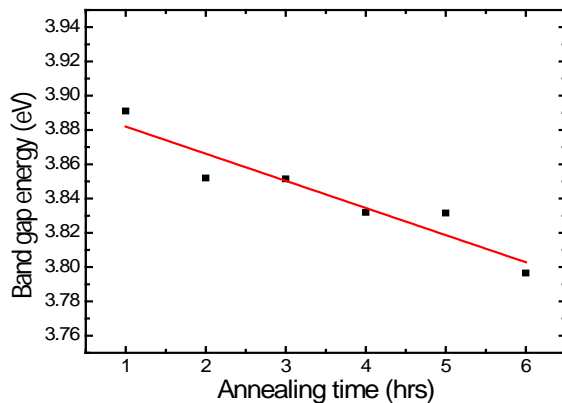**Figure 8.** Variation in Band gap energy with annealing time for TiO_2/Nb_2O_5 composite films annealed at 450.0 °C.

The effect of annealing (dwelling) time on optical band gap was studied by annealing the TiO_2/Nb_2O_5 composite thin films at 450.0°C for different dwelling times ranging from 1.0 and 6.0 hrs. The results are shown in Figure 8. It is observed that the band gap energies decrease linearly with increase in annealing time. This behaviour could be attributed to improvement in the crystalline structure of the TiO_2/Nb_2O_5 composite films with increase in annealing time. Such behaviour has also been reported in literature and this narrowing of the band gap is thought to be caused by the decrease in transitions due to reduction of the oxygen defect width as a result of air annealing which fills up the vacant oxygen levels [37].

3.4. Electrochemical Impedance Spectroscopy (EIS) Analysis

Electrochemical Impedance Spectroscopy (EIS) is widely used to investigate the dynamics of interfacial charge transfer process occurring in each component in DSSC. The electron transport in a DSSC encounters internal impedances at the three spatially separated interfaces formed by the FTO/TiO_2 contact, TiO_2/dye/electrolyte, and electrolyte/Pt-PTO. The frequency response of the impedance at these interfaces can be analyzed by the Nyquist diagram and the lifetime of the electron in TiO_2 photoanode can be calculated from Bode phase plots [33]. Nyquist diagram features typically three semicircles, that in the order of increasing frequency are attributed to the Nernst diffusion within the electrolyte, the intermediate semi-circle corresponds to the electron transfer resistance/recombination at the TiO_2/electrolyte interface, while the third corresponds to the redox reaction at the platinum counter electrode [33,38]. The Bode phase features three characteristic frequency peaks in low-frequency, mid-frequency and high-frequency range according to those three processes respectively. The electron recombination lifetime (τ_n) within the TiO_2 photoanode can be calculated from the maximum angular frequency (ω_{max}) of the impendence semicircle arc at middle frequencies according to the relation [38,39].

$$\tau_n = \frac{1}{\omega_{max}} = \frac{1}{2\pi f_{max}} \qquad (4)$$

where f_{max} is the maximum peak frequency.

Figure 9 shows the Nyquist and Bode plots of DSSC based on TiO_2/Nb_2O_5 composites of varying thickness. It can be seen (Figure 9a) that the EIS exhibits only one major semicircle in intermediate-frequency regime. The radius of this semicircle represents the impedance due to electron transfer from the conduction band of the TiO_2 film to I_3^- in the electrolyte. It is observed that thicker films exhibit progressively larger radius of the semi-circle compared to thinner films, an indication that the charge-transfer resistance (or the so-called recombination resistance), R_R at the TiO_2/dye/electrolyte interface increases with increase in film thickness, resulting in decreased J_{SC} (Figure 4) and consequently, reduced power conversion efficiency in thicker films.

It is further observed that the central semicircles (Figure 9) are skewed to the positive side of the real impedance indicating that the charge transport resistance (R_T) in

TiO_2/Nb_2O_5 composite films was less than the charge transfer/recombination resistance (R_R). The absence of the arc in the low frequency region could mean the mass transport impedance (Z_d) due to Nernst diffusion of tri-iodide species in the electrolyte was negligible in this case. This factor could be explained by use of high performing electrolytes in cell fabrication. Also not evident are the arcs associated with high frequency regions where impedance contributions originate from the double-layer capacitances and the platinum coated-counter-electrode transfer resistances. This could be related to the small currents flowing through the complete cell thus causing little diffusion effects.
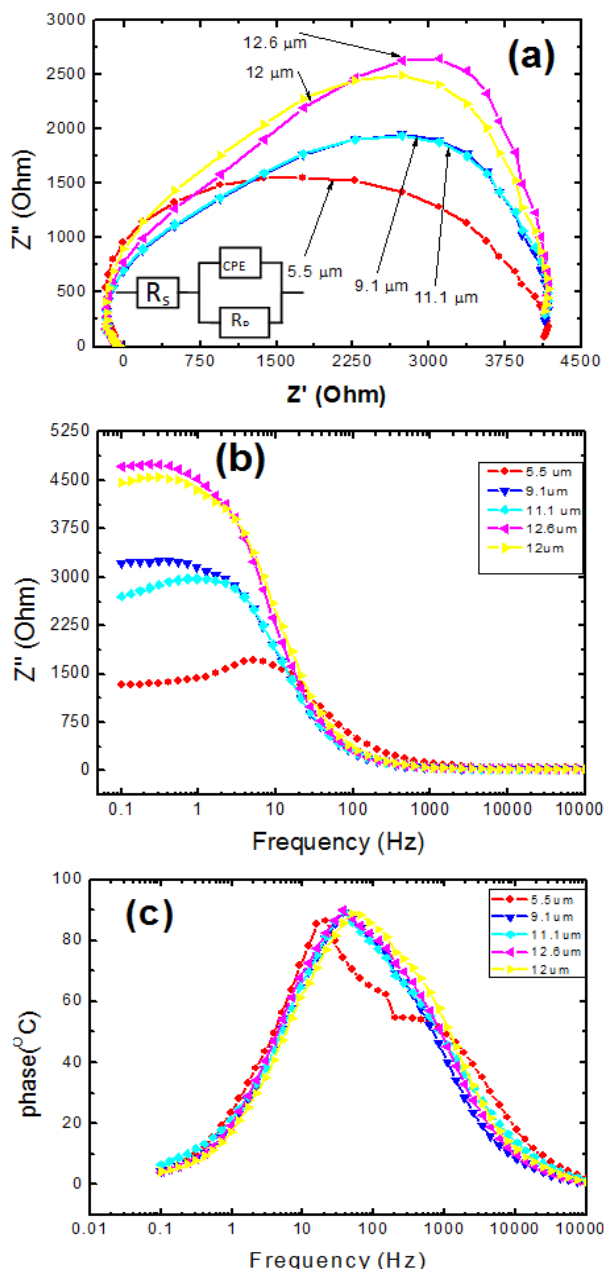

Figure 9. (a) Nyquist plot. Inset is the equivalent circuit (b) Bode plot and (c) Bode phase plots of DSSC assembled using TiO_2/Nb_2O_5 composite electrode films. The cells were subjected to 0.5V forward biasing

This shape of Nyquist plot with only one arc demonstrates evidence of the Gerischer impedance where, the Nyquist plot reduces to one main arc generated by parallel arrangement of charge-transfer resistance (R_R) and the chemical capacitance (C_μ) of TiO_2 film/electrolyte interface. The presence of Gerischer impedance confirms that the electron recombination reaction is faster than the transport of charge carriers through the film. This fact can explain why measured short circuit currents were very low, thus contributing to low conversion efficiencies (Figure 5).

Inset in Figure 9(a) shows the equivalent circuit consisting of a series resistance (R_S), parallel resistance (R_P) and chemical capacitance (C_μ) represented by constant phase element (*CPE*). The series resistance (R_S) represents the sum of TCO resistance, charge-transfer resistance at counter electrode, and the diffusion resistance in electrolyte [39,40] while the parallel resistance (R_P) represents the charge-transfer/recombination resistances (R_R) at the TiO_2/dye/electrolyte interface. Figure 9b shows the Bode plot for photoelectrodes of various film thicknesses. It is observed that there is a shift of frequency peaks in order of increasing film thickness as well as the transition of the high impedance values at low frequencies (0.1-100Hz) to low impedances at high frequencies (100 - 10,000Hz). A similar trend is observed in Bode phase plots (Figure 9c). Table 3 lists the measured values of R_S, R_P, *CPE* and the calculated values of the electron lifetime (τ_n). It is observed that the electron lifetime decreases with increase in photoelectrode film thickness and this may be the reason for faster recombination in the cells with thicker photoelectrodes. The cells with photoelectrode of 5.5μm thickness yielded longer electron lifetime. Notably, our values of R_S and R_P, are large (in the KΩ range) compared to other authors [38,41] implying that our samples had high internal impedances most likely attributed to the strong bonding of the TiO_2 to the glass substrate.

Table 3. EIS data based on TiO_2/Nb_2O_5 DSSC photoelectrodes of varying thicknesses.

Thickness z (μm)	CPE (μF)	R_p (kΩ)	R_s (kΩ)	τ (ms)
5.5	6.627	4.532	4.507	5.08
9.1	6.633	4.531	4.507	2.86
11.1	9.295	5.949	5.886	2.85
12.6	1.817	2.247	2.224	2.84
12	6.633	4.5`31	4.507	1.76

4. Conclusions

This paper presents the results of experimental study of Characterization of TiO_2/Nb_2O_5 composite thin films for Dye Sensitized Solar Cells prepared by the EPD method. Salient conclusions arising from the study are summarized as follows. Performance of DSSC is dependent on film thickness, which in turn is dependent on EPD deposition parameters. Higher deposition voltages are associated with rapid film deposition resulting in formation of agglomeration which reduces the optical transmittance. The highest optimal transmittance of 55.0 % at a wavelength (λ) of 1,300 nm was observed in film thickness of 5.5 μm deposited at 35.0 V for 90.0 s using a TiO_2/Nb_2O_5 ratio of 1:1 in a 2-propanol suspension solution.

The DSSC characteristics were dependent on film thickness. The highest open current voltage (V_{OC}) of 0.66 V, fill factor (FF) of 57.0%, short current density (J_{SC}) of 5.25 mA/cm^2 and photo conversion efficiency (PCE) of 2.0% was obtained with a film thickness of 5.5 μm. The band gap was found to be depended on annealing time duration and it decreased with increase in annealing time. The EIS analysis revealed that the charge transfer/ recombination resistance at the TiO$_2$/dye/ electrolyte interface increases with increase in film thickness. The electron lifetime was longer in cells with thinner photoelectrodes compared to thicker Photoelectrodes. It is therefore suggested that decreasing the film thickness could improve the charge recombination in DSSC as well as the electron transport properties.

Acknowledgements

References

[1]   T. Takamoto, M. Kaneiwa, M. Imaizumi, and M. Yamaguchi, "InGaP/GaAs-based multijunction solar cells," *Progress in Photovoltaics: Research and Applications,* vol. 13, pp. 495-511, 2005.

[2]   H. J. Snaith, "Estimating the maximum attainable efficiency in dye-sensitized solar cells," *Advanced Functional Materials,* vol. 20, pp. 13-19, 2010.

[3]   M. Grätzel, "Solar energy conversion by dye-sensitized photovoltaic cells," *Inorganic chemistry,* vol. 44, pp. 6841-6851, 2005.

[4]   B. Oregan and M. Gratzel, "A low-cost, high-efficiency solar-cell based on dye-sensitized colloidal tio2 films," Nature, Vol. 353, pp. 737-740, 1991.

[5]   E. Barea, X. Xu, V. Gonzalez-Pedro, T. Ripolles-Sanchis, "Origin of efficient enhancement in Nb$_2$O$_5$ coated titanium dioxide nanorod based dye sensitized solar cells," *Energy & Environmental Science*, vol 4. Pp. 3414-3418, 2011.

[6]   C. J. B. F. Padinger, T. Fromherz, J. C. Hummelen, and N. S. Sariciftci, "Fabrication of large area photovoltaic devices containing various blends of polymer and fullerene derivatives by using the doctor blade technique," *Opto-Electronics Review,,* vol. 8, pp. 280-283, 2000.

[7]   C.-S. Chou, Y.-J. Lin, R.-Y. Yang, and K.-H. Liu, "Preparation of TiO$_2$/NiO composite particles and their applications in dye-sensitized solar cells," *Advanced Powder Technology,* vol. 22, pp. 31-42, 2011.

[8]   K. Eguchi, H. Hoga, K. Sekizawa, and K. Sasaki, "Nb$_2$O$_5$- based composite electrodes for dye-sensitized solar cells," *Journal of the Ceramic Society Japan,* vol. 108, pp. 1067-1071, 2000.

[9]   S. M. Waita, B. O. Aduda, J. M. Mwabora, G. A. Niklasson, C. G. Granqvist and G. Boschloo, "Electrochemical characterization of TiO$_2$ blocking layers prepared by reactive DC magnetron sputtering," *Journal of Electroanalytical Chemistry,* vol. 637, pp. 79-83, 2009.

[10] S. Ito, T. N. Murakami, P. Comte, P. Liska, C. Grätzel, M. Nazeeruddin*, et al.*, "Fabrication of thin film dye sensitized solar cells with solar to electric power conversion efficiency over 10%," *Thin solid films,* vol. 516, pp. 4613-4619, 2008.

[11] L.-T. Yan, F.-L. Wu, L. Peng, L.-J. Zhang, P.-J. Li, S.-Y. Dou, *et al.*, "Photoanode of dye-sensitized solar cells based on a ZnO/TiO$_2$ composite film," *International Journal of Photoenergy,* vol. 2012, 2012.

[12] J.-H. Yum, S.-S. Kim, D.-Y. Kim, and Y.-E. Sung, "Electrophoretically deposited TiO$_2$ photo-electrodes for use in flexible dye-sensitized solar cells," *Journal of Photochemistry and Photobiology A: Chemistry,* vol. 173, pp. 1-6, 2005.

[13] J. Bandy, Q. Zhang, and G. Cao, "Electrophoretic deposition of titanium oxide nanoparticle films for dye-sensitized solar cell applications," *Materials Sciences and Applications,* vol. 2, pp. 1427, 2011.

[14] A. Boccacini and I. Zhitomisrky, "Application of electrophoretic and electrolytic deposition techniques in ceramic processing," *Current Opinion in Solid State and Material Science,* vol.6, pp. 257-260, 2002.

[15] O. Van der Biest and L. Vandeperre, "Electrophoretic deposition of materials," *Annual Reviews Material Science,* vol.29, no. 1, pp. 327-352, 1999.

[16] M. Kawakita, T. Uchikoshi, J. Kawakita, and Y. Sakka, "Preparation of crystalline-oriented Titania photoelectrodes on I-TO glasses from a 2-propanol-2,4-pentanedione solvent by electrophoretic deposition in a strong magnetic field," *Journal of the American Ceramic* Society, vol. 92, no. 5, pp. 984-989, 2009.

[17] B. Laxmidhar and L. Meilin, "A review on fundamentals and applications of electrophoretic deposition (EPD)," *Progress in Materials Science,* vol. 52, pp. 1-61, 2007.

[18] P. Sarkar and P. Nicholson, "Electrophoretic deposition. mechanism, kinetics and applications to ceramic*s*," *Journal American Ceramics Society*, vol. 79, no. 8, pp. 1987-2000, 1996.

[19] M. R. Narayan and A. Raturi, "Deposition and characterization of titanium dioxide films formed by electrophoretic deposition," *International Journal of Materials Engineering Innovation,* vol. 3, no. 1, pp. 17-31, 2012.

[20] S. Cabanas-Polo and A. Boccaccini, "Electrophoretic deposition of nanoscale TiO$_2$: technology and applications," *Journal of the European Ceramic Society*, 2015.

[21] R. Moreno and B. Ferarri, "Advanced ceramic via epd of aqueous slurries," *American Ceramic Society Bulletin,* Vol. 79, pp. 44-48. 2002.

[22] S. Radice, C. Bradbury, J. Michler and S. Michler, "Critical particle concentration in electrophoretic deposition, "*Journal of the European Ceramic Society*, vol. 30, no. 5, pp. 1079-1088, 2010.

[23] J. Van Tassel and C. Randall, "Mechanisms of electrophoretic deposition," *Key Engineering Materials,* vol. 314, pp. 167-174, 2006.

[24] L. Besra and M. Liu, "A review of fundamentals and applications of electrophoretic deposition (EPD)," *Progress in Materials Science*, vol. 52, no. 1, pp. 1-61, 2007.

[25] F. Nyongesa and B. O. Aduda, "Electrophoretic deposition of titanium dioxide thin films for photocatalytic water purification systems," *Advances in Materials, v*ol. 6, no. 4, pp. 31-37, 2017. doi: 10.11648/j.am.20170604.11

[26] J-Joon Lee, Md. Mahbubur Rahman, S. Sarker, N.C. D. Nath, A.J. S Ahammad and J. K. Lee, "Metal oxides and their composites for the photoelectrode of dye sensitized solar cells," *Advances in Composite Materials for Medicine and Nanotechnology*, Edited by Brahim Attaf (Ed.), ISBN: 978-953307-235-7, InTech, 2011.

[27] A. Le Viet, R. Jose, M. V. Reddy, B. V. R. Chowdari, and S. Ramakrishna, "Nb$_2$O$_5$ Photoelectrodes for Dye-Sensitized Solar Cells: Choice of the Polymorph," *Journal of Physical Chemistry C*, vol. 114, no. 49, pp. 21795-21800, 2010

[28] R. Jose, V. Thavasi, and S. Ramakrishna, "Metal oxides for dye-sensitized solar cells," *Journal of the American Ceramic Society,* vol. 92, pp. 289-301, 2009.

[29] L. C. Gould M., "Examination of the optical band gap of various semiconducting materials ," Reed College, Ed., ed. Portland, OR 97202, 2010.

[30] H. Chang, T.-J. Hsieh, T.-L. Chen, K.-D. Huang, C.-S. Jwo, and S.-H. & Chien, "Dye-sensitized solar cells made with TiO$_2$-coated multi-wall carbon nanotubes and natural dyes extracted from Ipomoea," *Materials transactions,* vol. 50, pp. 2879-2884, 2009.

[31] H. Su, Y. Huang, Y. Chang, P. Zhai, N. Y. Hau *et al*., "The synthesis of Nb-doped TiO$_2$ nanoparticles for improved-performance dye sensitized solar cells," *Electrochimica Acta*, vol. 182, pp. 230-237, 2015.

[32] N. Ghrairi and M. Bouaicha, "Structural, morphological, and optical properties of TiO$_2$ thin films synthesized by the electro phoretic deposition technique," *Nanoscale research letters,* vol. 7, pp. 1-7, 2012.

[33] H. I. Yavuz, "Design of high-efficiency dye-sensitized nanocrystalline solar cells, "PhD, Middle East Technical University, 2014.

[34] R. Oommen, P. Rajalakshmi, and S. Sudha, "Optical characteristics of TiO$_2$ thin films sensitized with the natural dye of Clitoria Ternatea," *Int. J. of Applied Phys & Math,* vol. 2, 2012.

[35] J. Sancho-Parramon and V. Janicki, "Effective medium theories for composite optical materials in spectral ranges of weak absorption: the case of Nb$_2$O$_5$–SiO$_2$ mixtures," *Journal of Physics D: Applied Physics,* vol. 41, p. 2153, 2008.

[36] J. C. G. Parakh, "Temperature dependent dielectric and electrical properties of Niobium(v)oxide," *Proc. Indian Naian Sci. Acad.,,* vol. 51, pp. 824-831, 1985.

[37] S. S. D. Kekuda, "Effect of annealing temperature on the structural and optical properties of Zinc Oxide (ZnO) thin films prepared by Spin coating process," *IOP Conf. Series: Materials Science and Engineering,* vol. 73, pp. 1-5, 2015.

[38] X. Tang, W. Yuxun and C. Guozhong, "Effect of the adsorbed concentration of dye on charge recombination in dye-sensitized solar cells," *Journal of Electroanalytical Chemistry*, vol. 694, pp. 6-11, 2013.

[39] X. Luo, J. Kim, J. Ahn, D. Lee, J. Kim and S. Kim, "Electrospraying-assisted rapid dye molecule uptake on TiO$_2$ nanoparticles for speeding up dye-sensitized solar cell fabrication," *Solar Energy Materials & Solar Cells*, vol. 144, pp. 411-417, 2016.

[40] F. Fabregat-Santiago, G. Garcia-Belmonte, I. Mora-Sero, and J. Bisquert, "Characterization of nanostructured hybrid and organic solar cells by impedance spectroscopy," *Phys. Chem. Chem. Phys,* vol. 13, pp. 9083-9118, 2011.

[41] J.-Chuan Chou, S.-Chang Lin, Y.-Hung Liao, "The influence of electrophoretic deposition for fabricating dye-sensitized solar cell," *Journal of Nanomaterials*, vol. 2014. 2014.